

Fuzzy dark matter soliton core hosting a supermassive black hole as a dense low-mass perturber in strong gravitational lensing

Masamune Oguri^{a,b} and Naoi Kubo^b

^aCenter for Frontier Science, Chiba University, 1-33 Yayoicho, Inage, Chiba 263-8522, Japan

^bDepartment of Physics, Graduate School of Science, Chiba University, 1-33 Yayoicho, Inage, Chiba 263-8522, Japan

E-mail: masamune.oguri@chiba-u.jp

Abstract. Recent high-resolution imaging observations of strong lens systems reveal dense low-mass perturbers. We propose a soliton core, whose central density is boosted by a supermassive black hole (SMBH), in the fuzzy dark matter (FDM) model as an efficient perturber in strong gravitational lensing. The higher central density makes it less efficient in the tidal mass loss, and leads to the higher impact in gravitational lensing. We show that the mass profile of a $\sim 10^6 M_\odot$ perturber in JVAS B1938+666, which does not resemble any known astronomical object, can be well explained by a soliton core in the FDM model with the mass of $4 \times 10^{-21} \text{ eV}$ hosting an SMBH with the mass of $4 \times 10^5 M_\odot$. The high mass of the SMBH may be explained by several scenarios that predict heavy SMBH seeds such as the direct collapse black hole formation and primordial black holes.

Keywords: dark matter, gravitational lensing, supermassive black holes

Contents

1	Introduction	1
2	Properties of soliton cores	2
2.1	Generic properties	2
2.2	Low-mass perturber in JVAS B1938+666	2
3	Possible scenarios	4
3.1	FDM mass and halo mass	4
3.2	Tidal mass loss scenario	4
3.3	Heavy SMBH seed scenario	6
4	Summary	7

1 Introduction

The observation of the distribution of dark matter at the small scale provides an important clue to the nature of dark matter [1]. Strong gravitational lensing serves as one of the most powerful methods to constrain the dark matter distribution at the very small scale. Recently, by making use of the so-called gravitational imaging technique [2], Refs. [3, 4] claim the significant detection of a dark object, which perturbs the observed shape of the lensed arc, with the mass of $\sim 10^6 M_\odot$ toward the strong lens system JVAS B1938+666, with the significance of $\sim 26\sigma$. The mass profile of the perturber is studied in detail in Ref. [5], which concludes that the mass profile of the perturber is best fitted by a two component model consisting of a point-mass object and an extended object with a nearly constant surface density out to a truncation radius of ~ 140 pc. It is argued that the mass profile does not resemble that of any known astronomical object, and may be explained by self-interacting dark matter with the large effective cross-section of $\gtrsim 800 \text{ cm}^2 \text{g}^{-1}$ [5]. The detection of a similarly compact perturber in another strong lens system [6, 7] may suggest that such dark compact perturbers are ubiquitous.

In this paper, we argue that the mass profile of the $\sim 10^6 M_\odot$ perturber in JVAS B1938+666 can be naturally explained in the fuzzy dark matter (FDM) scenario [8–10]. In this scenario, the point mass and the extended components are explained by a supermassive black hole (SMBH) and a soliton core, respectively. We discuss parameters that reproduce the observed mass profile. While Ref. [11] also discusses a soliton core as a possible origin of dense perturbers in strong lens systems, our analysis differs from Ref. [11] in that we consider the effect the SMBH that can significantly affect the mass profile of the soliton core.

This paper is organized as follows. In Sec. 2, we summarize basic properties of soliton cores and discuss parameters that explain the $\sim 10^6 M_\odot$ perturber in JVAS B1938+666. We discuss possible scenarios for the origin of the $\sim 10^6 M_\odot$ perturber in Sec. 3. Finally we give a summary in Sec. 4. Throughout the paper we assume a flat Universe with the matter density parameter $\Omega_m = 0.3156$, the baryon density parameter $\Omega_b = 0.05$, the dimensionless Hubble constant $h = 0.6727$, the spectral index $n_s = 0.96$, and the normalization of the matter power spectrum $\sigma_8 = 0.81$.

2 Properties of soliton cores

2.1 Generic properties

The governing equation of the structure formation in the FDM model is the Schrödinger-Poisson equation. The soliton core, which is seen in cosmological FDM simulations, corresponds to the ground state solution of the Schrödinger-Poisson equation. A commonly used fitting form of the density profile of the soliton core is [9, 10]

$$\rho_{\text{sol}}(r) = \frac{\rho_c}{\{1 + 0.091(r/r_c)^2\}^8}, \quad (2.1)$$

where ρ_c is given by

$$\rho_c = 0.019a^{-1} \left(\frac{mc^2}{10^{-22} \text{ eV}} \right)^{-2} \left(\frac{r_c}{\text{kpc}} \right)^{-4} M_\odot \text{pc}^{-3}, \quad (2.2)$$

with a being the scale factor and m being the mass of the FDM particle. The core radius r_c is known to scale with the halo mass M_h as [10]

$$r_c = 1.6g(z) \left(\frac{mc^2}{10^{-22} \text{ eV}} \right)^{-1} \left(\frac{M_h}{10^9 M_\odot} \right)^{-1/3} \text{kpc}, \quad (2.3)$$

$$g(z) = a^{1/2} \left(\frac{\zeta(z)}{\zeta(0)} \right)^{-1/6}, \quad (2.4)$$

and $\zeta(z)$ is the virial overdensity. At the lens redshift of JVAS B1938+666, its value is $g(0.881) \simeq 0.79$. The total mass of the soliton core is computed as

$$M_{\text{sol}} = \int_0^\infty \rho_{\text{sol}}(r) 4\pi r^2 dr \simeq 2.2 \times 10^8 a^{-1} \left(\frac{mc^2}{10^{-22} \text{ eV}} \right)^{-2} \left(\frac{r_c}{\text{kpc}} \right)^{-1} M_\odot. \quad (2.5)$$

By plugging Eq. (2.3) into the above equation and adopting the lens redshift $z = 0.881$, we obtain

$$M_{\text{sol}} = 3.3 \times 10^8 \left(\frac{mc^2}{10^{-22} \text{ eV}} \right)^{-1} \left(\frac{M_h}{10^9 M_\odot} \right)^{1/3} M_\odot. \quad (2.6)$$

We note that, from Eq. (2.1), the cylindrical mass profile within the projected radius R is computed as

$$M_{\text{cyl}}(< R) = M_{\text{sol}} \left[1 - \frac{1}{\{1 + 0.091(R/r_c)^2\}^{13/2}} \right], \quad (2.7)$$

which behaves as $M_{\text{cyl}}(< R) \propto R^2$ at $R \ll r_c$ and $M_{\text{cyl}}(< R) \rightarrow M_{\text{sol}}$ at $R \rightarrow \infty$.

2.2 Low-mass perturber in JVAS B1938+666

In the case of the $\sim 10^6 M_\odot$ perturber in JVAS B1938+666, the best-fitting model ('UD+PM' model) indicates the the mass of the point-mass component of $M_{\text{PM}} = (4.25 \pm 0.21) \times 10^5 M_\odot$ and the mass of the extended component of $M_{\text{UD}} = (1.76 \pm 0.10) \times 10^6 M_\odot$ [5]. By interpreting them as an SMBH and a soliton core, respectively, their mass ratio $M_{\text{SMBH}}/M_{\text{sol}} \simeq 0.24$ is accurately known from the observation, indicating that the effect of the SMBH on the mass profile of the soliton core for this case can be evaluated quantitatively. The effect of an SMBH

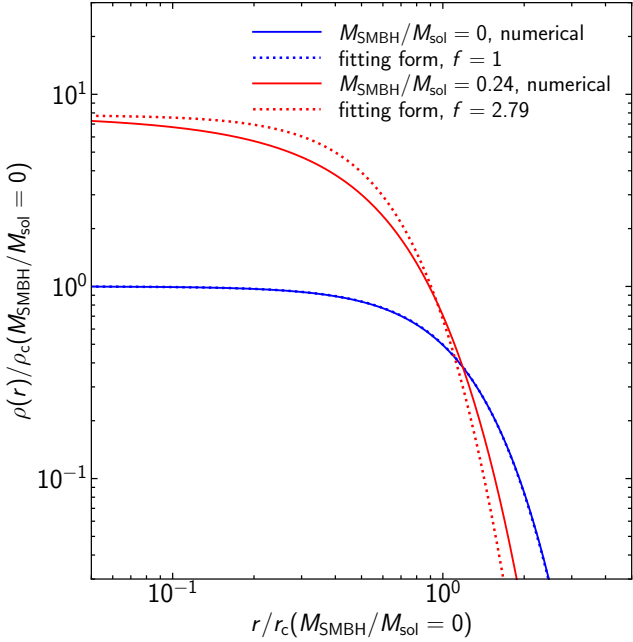


Figure 1. Mass profiles of the soliton core with (red) and without (blue) an SMBH with the ratio of the mass of the SMBH to that of the soliton core of $M_{\text{SMBH}}/M_{\text{sol}} = 0.24$. Dotted lines indicate the fitting from given by Eq. (2.1) with the transformation of $\rho_{\text{sol}}(r) \rightarrow f^2 \rho_{\text{sol}}(f^{2/3}r)$ with $f = 1$ and 2.79 for the case without and with an SMBH, respectively.

on the soliton core is studied in detail in Ref. [12], which we follow to solve the Schrödinger-Poisson equation with an SMBH potential numerically, using the shooting method, to obtain the mass profile.

Fig. 1 compares mass profiles of the soliton core with and without an SMBH, assuming that the total mass of the soliton core is same for both cases. It is seen that the presence of an SMBH enhances the gravitational attractive force to make the soliton core more compact. Without an SMBH, we confirm that Eq. (2.1) very well reproduces the numerical solution. Here we consider the transformation $\rho_{\text{sol}}(r) \rightarrow f^2 \rho_{\text{sol}}(f^{2/3}r)$, which conserves the total mass M_{sol} , to check such a transformed profile can reproduce the numerical solution for the case of $M_{\text{SMBH}}/M_{\text{sol}} = 0.24$. By choosing $f = 2.79$ that corresponds to the value at $r \rightarrow 0$, we find that the transformed version of Eq. (2.1) reproduces the numerical solution reasonably well. This analysis suggests that the core radius of the soliton core is reduced by a factor of $f^{-2/3} \simeq 0.50$ due to the presence of the SMBH with the mass ratio of $M_{\text{SMBH}}/M_{\text{sol}} = 0.24$.

We then compare the cylindrical mass $M_{\text{cyl}}(< R)$, which is defined by the total mass of the lens within the projected radius R , for our SMBH plus a soliton core model to check parameters that reproduce the observed mass profile of the $\sim 10^6 M_{\odot}$ perturber in JVAS B1938+666. We choose $M_{\text{SMBH}} = M_{\text{PM}}$ and $M_{\text{sol}} = M_{\text{UD}}$, assume Eq. (2.1) for the density profile of the soliton core, and check what core radius r_c can reproduce the observed mass profile. The comparison in Fig. 2 suggests that the core radius of $r_c \simeq 90$ pc reproduces the best-fitting UD+PM model reasonably well. Therefore, in the following analysis, we adopt $r_{c,\text{obs}} = 90$ pc and explore scenarios that reproduce both M_{UD} and $r_{c,\text{obs}}$.

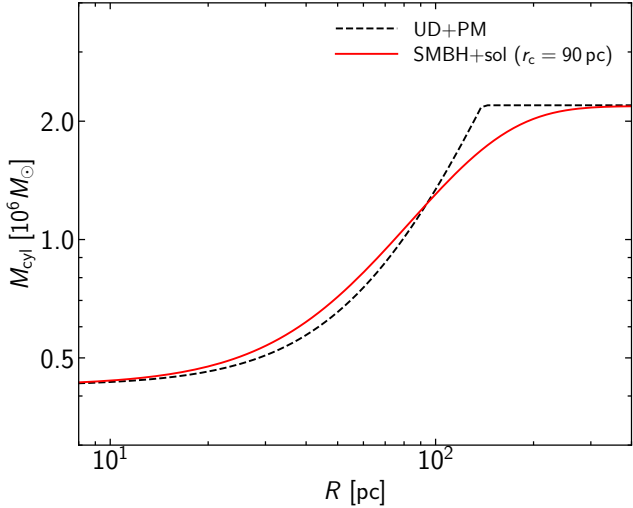


Figure 2. The cylindrical mass $M_{\text{cyl}}(< R)$ as a function of the projected radius R for the UD+PM model, which corresponds to the best-fitting model in Ref. [5], as well as $M_{\text{cyl}}(< R)$ for an SMBH plus a soliton core in the FDM model. We choose $M_{\text{SMBH}} = M_{\text{PM}}$, $M_{\text{sol}} = M_{\text{UD}}$, and $r_c = 90$ pc.

3 Possible scenarios

3.1 FDM mass and halo mass

Here we discuss possible scenarios for the origin of the $\sim 10^6 M_\odot$ perturber in JVAS B1938+666. Based on the comparison shown in Fig. 2, we assume $M_{\text{sol}} = M_{\text{UD}}$ and $f^{-2/3}r_c = r_{\text{c,obs}}$, where $f = 2.79$ accounts for the shrinking of the soliton core due to the SMBH for this perturber, and use Eqs. (2.6) and (2.3) to obtain the FDM mass mc^2 and the halo mass M_h , which we refer to as the mass of a subhalo hosting the soliton core and an SMBH and acting as the perturber in JVAS B1938+666, that reproduce the observed mass profile, finding $mc^2 \simeq 3.6 \times 10^{-21} \text{ eV}$ and $M_h \simeq 7.1 \times 10^6 M_\odot$ as shown in Fig. 3.

A potential issue is that the SMBH mass of $M_{\text{SMBH}} \simeq 4 \times 10^5 M_\odot$ may be too high compared with the (sub)halo mass of $M_h \simeq 7.1 \times 10^6 M_\odot$. For comparison, the SMBH mass–halo mass relation constrained from observations (e.g., [13]) predicts that the halo mass corresponding to $M_{\text{SMBH}} \simeq 4 \times 10^5 M_\odot$ is $M_h \sim 10^{11} M_\odot$, which is much higher than the halo mass needed to explain the soliton core.

3.2 Tidal mass loss scenario

A possible way to explain the high SMBH mass is to consider the mass loss of the soliton core due to the tidal effect [14]. Once the halo that hosts the soliton core and the SMBH enters the main halo that is responsible for the primary strong lensing of JVAS B1938+666, the tidal force acting on the soliton core affects the total mass and the density profile of the soliton core. In previous studies (e.g., [14]), it is shown that the density profile of the soliton core after the mass loss due to the tidal evolution is still approximately given by Eq. (2.1). As a result, the effect of the tidal evolution can be approximated by the transformation $M_{\text{sol}} \rightarrow \lambda M_{\text{sol}}$ and $r_c \rightarrow \lambda^{-1} M_{\text{sol}}$ with $\lambda < 1$. Since the central density is changed as $\rho_{\text{sol}}(0) \rightarrow \lambda^4 \rho_{\text{sol}}(0)$, the tidal mass loss makes the soliton core less dense and more extended. By computing $M_{\text{sol}} = M_{\text{UD}}$ and $f^{-2/3}r_c = r_{\text{c,obs}}$ after the transformation, it is easily shown

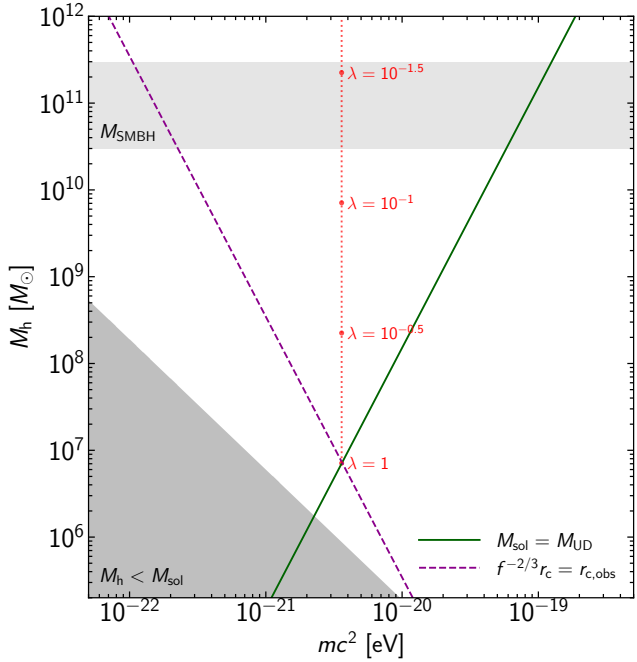


Figure 3. The FDM mass mc^2 and the halo mass M_h that explain the $\sim 10^6 M_\odot$ perturber in JVAS B1938+666. The dark shaded region is a forbidden region defined by $M_h < M_{\text{sol}}$. The filled point for $\lambda = 1$ indicates the parameters that explain the observation in the absence of any tidal mass loss of the soliton core. The dotted line shows a track for different values of λ that is defined by the ratio of the soliton core masses after and before the tidal mass loss. The light shaded region indicates a rough range of the halo mass that is consistent with the SMBH mass of $M_{\text{SMBH}} = 4.25 \times 10^5 M_\odot$ based on the extrapolation of the SMBH mass–halo mass from higher masses.

that the effect of the mass loss can increase the halo mass M_h while the FDM mass mc^2 is unchanged. Fig. 3 indicates that we may be able to explain both the SMBH mass and the mass profile of the soliton core simultaneously with $\lambda \sim 10^{-1.2} - 10^{-1.5}$.

We can use the result in Ref. [14] to estimate the efficiency of the mass loss of the soliton core. From Eq. (2.2), we estimate the central density of the soliton core without the gravitational effect of the SMBH to $\rho_{\text{sol}}(0) = 0.025\lambda^{-4} M_\odot \text{pc}^{-3}$. In contrast, assuming the virial mass of the main lensing halo of JVAS B1938+666 to $10^{13} M_\odot$ [15] and adopting the mass-concentration relation in Ref. [16], the halo density is $\bar{\rho} = 1.3 \times 10^{-5} M_\odot \text{pc}^{-3}$ at the virial radius and $\bar{\rho} = 0.042 M_\odot \text{pc}^{-3}$ at 1% of the virial radius that roughly corresponds to the Einstein radius. Therefore, for $\lambda < 0.1$, the ratio of the central density of the soliton core to the halo density is $\mu = \rho_{\text{sol}}(0)/\bar{\rho} > 6 \times 10^6$ for that range of radii. Since the tidal mass loss is not significant for $\mu \gtrsim 70$ [14], we conclude that the mass loss scenario face difficulties in the lack of an efficient mass loss. In addition, the abundance of massive subhalos is much smaller compared with that of lower mass subhalos. Considering the discussion on the abundance of the perturber in Ref. [5] that the the observed abundance is in agreement with the abundance of $10^6 - 10^7 M_\odot$ subhalos in the standard cold dark matter (CDM) scenario, the mass loss scenario also has difficulties in explaining the observed abundance.

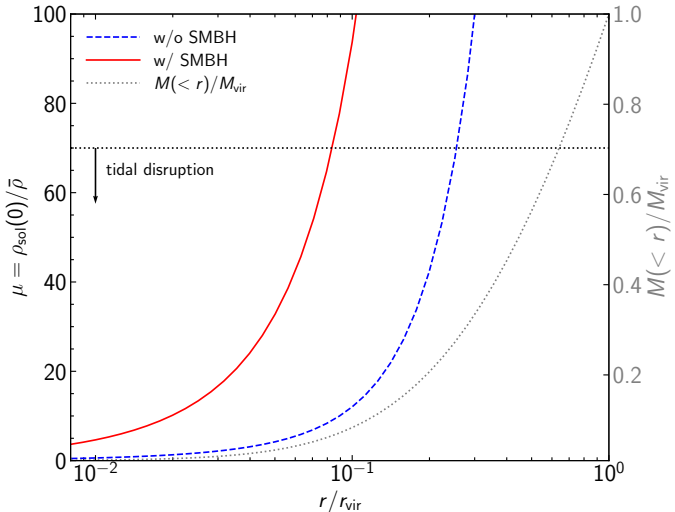


Figure 4. The density ratio $\mu = \rho_{\text{sol}}(0)/\bar{\rho}$ between the central density of the soliton core with (solid) and without (dashed) the SMBH and the density of the main halo as a function of the distance r/r_{vir} of the soliton core from the center of the main halo. The horizontal dotted line indicates the rough condition for the tidal disruption, $\mu \lesssim 70$ [14]. The gray dotted line shows the enclosed mass fraction $M(< r)/M_{\text{vir}}$ of the main halo as a function of r/r_{vir} .

3.3 Heavy SMBH seed scenario

We consider another scenario to explain the high SMBH mass, given the fact that the current SMBH mass–halo mass relation is based on observations of black holes with SMBH masses of $\gtrsim 10^7 M_{\odot}$, and hence the discussion above relies on the extrapolation of the SMBH mass–halo mass relation down to lower masses. Since the origin of SMBHs is yet to be understood, it is possible that low mass halos host SMBHs that are much more massive than predicted by the extrapolation of the SMBH mass–halo mass relation. High SMBH masses in low mass halos can be naturally explained in several scenarios for the origin of SMBHs, including the direct collapse black hole formation (e.g., [17, 18]) and primordial black holes (e.g., [19, 20]). Such heavy SMBH seeds may also be suggested by recent discoveries of little red dots at high redshift (see e.g., [21] for a review). The presence of an SMBH with $M_{\text{SMBH}} \sim 10^5 M_{\odot}$ in a halo with $M_{\text{h}} \sim 10^7 M_{\odot}$ may be possible in such scenarios. The observed abundance of the perturber can also be naturally explained for those scenarios given the low halo mass.

Here we discuss the efficiency of the tidal mass loss for the soliton core hosting the SMBH. As is clear from Fig. 1, the presence of the SMBH whose mass is comparable to the soliton core can significantly enhance the central density of the soliton core, by a factor of $f^2 \simeq 7.8$, to make the mass loss much more inefficient. In Fig. 4, we compare the density ratios $\mu = \rho_{\text{sol}}(0)/\bar{\rho}$ of soliton cores with $M_{\text{sol}} = M_{\text{UD}}$ with and without the SMBH as a function of their position within the main halo. Assuming that the soliton cores are tidally disrupted for $\mu \lesssim 70$, we find that the soliton cores survive at $r/r_{\text{vir}} \gtrsim 0.08$ and $\gtrsim 0.3$ with and without the SMBH, respectively. While this analysis suggests that the soliton core, even with the SMBH, is difficult to survive near the Einstein radius of $r/r_{\text{vir}} \sim 0.01$, we emphasize that strong lensing perturbers can reside in the outskirt of the lensing halo as long as their projected separation from the lens center is small. By checking the enclosed mass fraction $M(< r)/M_{\text{vir}}$ of the main halo, this result indicates that roughly $\sim 5\%$ and $\sim 30\%$ of the

soliton cores with and without the SMBH are tidally disrupted, respectively. This analysis indicates that soliton cores with central SMBHs are more likely to survive when they accrete onto massive halos and they can be located closer to the center of the main halo.

We note that here we implicitly assume that the effect of the tidal mass loss is characterized by the density ratio μ alone even in the presence of the SMBH. Checking the validity of such assumption is left for future work.

4 Summary

Ref. [5] argues that the mass profile of the $\sim 10^6 M_\odot$ perturber in JVAS B1938+666 does not resemble that of any known astronomical object. We advocate that the mass profile is naturally explained by considering a soliton core in the FDM model hosting an SMBH. We have found that, given the observed mass ratio of the point mass and extended components, the gravitational force of the SMBH affects the mass profile of the soliton core such that its core radius is reduced by a factor of ~ 2 and its central density is enhanced by a factor of ~ 8 . The observed mass profile of the soliton core is explained by the FDM mass of $mc^2 \simeq 3.6 \times 10^{-21} \text{ eV}$ and the halo mass of $M_h \simeq 7.1 \times 10^6 M_\odot$. The halo mass is small compared with the mass of the SMBH of $M_{\text{SMBH}} = 4.25 \times 10^5 M_\odot$, which may be reconciled for some scenarios that predict heavy SMBH seeds, such as the direct collapse black hole formation and primordial black holes.

We note that are several caveats in this work. First, there are several observations that tightly constrain the FDM model such that the FDM model cannot explain all the dark matter for a wide range of the FDM mass (e.g., [22] for a review). Therefore the scenario proposed in this paper may not work as it is, and some modifications such as a compound dark matter model consisting of the FDM and other form of dark matter, considering the two-field (or multi-field) FDM model, or including the self-interaction of the FDM may be needed [22]. Second, discussions in this paper rely on the relation between the soliton core mass and the halo mass in Ref. [10], which is subject to various uncertainties and diversities (e.g., [23–25]). Third, other systematic effects such as uncertainties of the estimation of the tidal mass loss [26] and baryonic effects should also affect our quantitative result.

Despite these caveats, we expect that our argument that a soliton core in the FDM model serves as a more efficient perturber in a strong lens system when it hosts an SMBH at the center generically holds. Since the SMBH enhances the central density of the soliton core, it is less easily disrupted by the tidal effect and its lensing effect is more significant. Such dens low-mass perturbers will affect strong lensing observables in several ways, including flux ratio anomalies (e.g., [27]) and positional anomalies (e.g., [28]). We leave the exploration along this line to future work.

Acknowledgments

This work was supported by JSPS KAKENHI Grant Numbers JP25H00662, JP25H00672.

References

- [1] J.S. Bullock and M. Boylan-Kolchin, *Small-Scale Challenges to the Λ CDM Paradigm*, *ARA&A* **55** (2017) 343 [[1707.04256](#)].
- [2] L.V.E. Koopmans, *Gravitational imaging of cold dark matter substructures*, *MNRAS* **363** (2005) 1136 [[astro-ph/0501324](#)].

- [3] D.M. Powell, J.P. McKean, S. Vegetti, C. Springola, S.D.M. White and C.D. Fassnacht, *A million-solar-mass object detected at a cosmological distance using gravitational imaging*, *Nature Astronomy* **9** (2025) 1714 [[2510.07382](#)].
- [4] J.P. McKean, C. Springola, D.M. Powell and S. Vegetti, *An extended and extremely thin gravitational arc from a lensed compact symmetric object at redshift of 2.059*, *MNRAS* **544** (2025) L24 [[2510.07386](#)].
- [5] S. Vegetti, S.D.M. White, J.P. McKean, D.M. Powell, C. Springola, D. Massari et al., *A possible challenge for Cold and Warm Dark Matter*, *arXiv e-prints* (2026) arXiv:2601.02466 [[2601.02466](#)].
- [6] Q. Minor, S. Gad-Nasr, M. Kaplinghat and S. Vegetti, *An unexpected high concentration for the dark substructure in the gravitational lens SDSSJ0946+1006*, *MNRAS* **507** (2021) 1662 [[2011.10627](#)].
- [7] W.J.R. Enzi, C.M. Krawczyk, D.J. Ballard and T.E. Collett, *The overconcentrated dark halo in the strong lens SDSS J0946 + 1006 is a subhalo: evidence for self-interacting dark matter?*, *MNRAS* **540** (2025) 247 [[2411.08565](#)].
- [8] W. Hu, R. Barkana and A. Gruzinov, *Fuzzy Cold Dark Matter: The Wave Properties of Ultralight Particles*, *Phys. Rev. Lett.* **85** (2000) 1158 [[astro-ph/0003365](#)].
- [9] H.-Y. Schive, T. Chiueh and T. Broadhurst, *Cosmic structure as the quantum interference of a coherent dark wave*, *Nature Physics* **10** (2014) 496 [[1406.6586](#)].
- [10] H.-Y. Schive, M.-H. Liao, T.-P. Woo, S.-K. Wong, T. Chiueh, T. Broadhurst et al., *Understanding the Core-Halo Relation of Quantum Wave Dark Matter from 3D Simulations*, *Phys. Rev. Lett.* **113** (2014) 261302 [[1407.7762](#)].
- [11] L. Lei, Y.-Y. Wang, Q. Li, J. Dong, Z.-F. Wang, W.-L. Lin et al., *A Dense Dark Matter Core of the Subhalo in the Strong Lensing System JVAS B1938+666*, *ApJ* **991** (2025) L27 [[2509.07808](#)].
- [12] E.Y. Davies and P. Mocz, *Fuzzy dark matter soliton cores around supermassive black holes*, *MNRAS* **492** (2020) 5721 [[1908.04790](#)].
- [13] H. Zhang, P. Behroozi, M. Volonteri, J. Silk, X. Fan, P.F. Hopkins et al., *TRINITY I: self-consistently modelling the dark matter halo-galaxy-supermassive black hole connection from $z = 0\text{--}10$* , *MNRAS* **518** (2023) 2123 [[2105.10474](#)].
- [14] X. Du, B. Schwabe, J.C. Niemeyer and D. Bürger, *Tidal disruption of fuzzy dark matter subhalo cores*, *Phys. Rev. D* **97** (2018) 063507 [[1801.04864](#)].
- [15] M. Oguri, C.E. Rusu and E.E. Falco, *The stellar and dark matter distributions in elliptical galaxies from the ensemble of strong gravitational lenses*, *MNRAS* **439** (2014) 2494 [[1309.5408](#)].
- [16] B. Diemer and M. Joyce, *An Accurate Physical Model for Halo Concentrations*, *ApJ* **871** (2019) 168 [[1809.07326](#)].
- [17] K. Omukai, *Primordial Star Formation under Far-Ultraviolet Radiation*, *ApJ* **546** (2001) 635 [[astro-ph/0011446](#)].
- [18] V. Bromm and A. Loeb, *Formation of the First Supermassive Black Holes*, *ApJ* **596** (2003) 34 [[astro-ph/0212400](#)].
- [19] N. Cappelluti, G. Hasinger and P. Natarajan, *Exploring the High-redshift PBH- Λ CDM Universe: Early Black Hole Seeding, the First Stars and Cosmic Radiation Backgrounds*, *ApJ* **926** (2022) 205 [[2109.08701](#)].
- [20] S. Zhang, B. Liu and V. Bromm, *A Novel Formation Channel for Supermassive Black Hole Binaries in the Early Universe via Primordial Black Holes*, *ApJ* **992** (2025) 136 [[2508.00774](#)].

- [21] K. Inayoshi and L.C. Ho, *A Critical Evaluation of the Physical Nature of the Little Red Dots*, *arXiv e-prints* (2025) arXiv:2512.03130 [2512.03130].
- [22] A. Eberhardt and E.G.M. Ferreira, *Ultralight fuzzy dark matter review*, *arXiv e-prints* (2025) arXiv:2507.00705 [2507.00705].
- [23] S. May and V. Springel, *Structure formation in large-volume cosmological simulations of fuzzy dark matter: impact of the non-linear dynamics*, *MNRAS* **506** (2021) 2603 [2101.01828].
- [24] M. Nori and M. Baldi, *Scaling relations of fuzzy dark matter haloes - I. Individual systems in their cosmological environment*, *MNRAS* **501** (2021) 1539 [2007.01316].
- [25] H.Y.J. Chan, E.G.M. Ferreira, S. May, K. Hayashi and M. Chiba, *The diversity of core-halo structure in the fuzzy dark matter model*, *MNRAS* **511** (2022) 943 [2110.11882].
- [26] H.Y.J. Chan, H.-Y. Schive, V.H. Robles, A. Kunkel, G.-M. Su and P.-Y. Liao, *Cosmological zoom-in simulation of fuzzy dark matter down to $z = 0$: tidal evolution of subhaloes in a Milky Way-sized halo*, *MNRAS* **540** (2025) 2653 [2504.10387].
- [27] D. Gilman, S. Birrer, A. Nierenberg, T. Treu, X. Du and A. Benson, *Warm dark matter chills out: constraints on the halo mass function and the free-streaming length of dark matter with eight quadruple-image strong gravitational lenses*, *MNRAS* **491** (2020) 6077 [1908.06983].
- [28] A. Amruth, T. Broadhurst, J. Lim, M. Oguri, G.F. Smoot, J.M. Diego et al., *Einstein rings modulated by wavelike dark matter from anomalies in gravitationally lensed images*, *Nature Astronomy* **7** (2023) 736 [2304.09895].